



Silica nanoparticles enhance disease resistance in *Arabidopsis* plants

Mohamed El-Shetehy^{1,2}✉, Aboubakr Moradi¹, Mattia Maceroni¹, Didier Reinhardt¹, Alke Petri-Fink^{1,3,4}, Barbara Rothen-Rutishauser¹, Felix Mauch¹ and Fabienne Schwab¹✉

In plants, pathogen attack can induce an immune response known as systemic acquired resistance that protects against a broad spectrum of pathogens. In the search for safer agrochemicals, silica nanoparticles (SiO_2 NPs; food additive E551) have recently been proposed as a new tool. However, initial results are controversial, and the molecular mechanisms of SiO_2 NP-induced disease resistance are unknown. Here we show that SiO_2 NPs, as well as soluble Si(OH)_4 , can induce systemic acquired resistance in a dose-dependent manner, which involves the defence hormone salicylic acid. Nanoparticle uptake and action occurred exclusively through the stomata (leaf pores facilitating gas exchange) and involved extracellular adsorption in the air spaces in the spongy mesophyll of the leaf. In contrast to the treatment with SiO_2 NPs, the induction of systemic acquired resistance by Si(OH)_4 was problematic since high Si(OH)_4 concentrations caused stress. We conclude that SiO_2 NPs have the potential to serve as an inexpensive, highly efficient, safe and sustainable alternative for plant disease protection.

Nanoagrochemicals are a promising tool to improve crop yield and thus global food security¹. Silica nanoparticles (SiO_2 NPs) have been proposed for the controlled nanodelivery of silicon (Si) and other active ingredients to plants, but they have never been systematically tested for this purpose. Si from orthosilicic acid (Si(OH)_4 , also known as monosilicic acid)—the hydrolytic degradation product of SiO_2 NPs—is the only known form of Si bioavailable for plants, and it is ubiquitous in soil pore water^{2–4}. Si(OH)_4 can promote plant growth and plant resistance against biotic and abiotic stresses^{3,5}, thereby protecting plants against pathogen attacks or agricultural damages related to severe climate conditions^{3,6,7}. The uptake and movement of SiO_2 NPs as well as other engineered nanomaterials in plants have been intensively studied in the past decade^{7–10}. However, it is uncertain how the nanoparticles interact with leaves at the subcellular level. Direct evidence by nanometre-resolution imaging for the entrance of intact nanoparticles into leaves, or the intercellular movement of SiO_2 NPs within leaves, is mostly missing¹⁰. It is also not known whether SiO_2 NPs can induce resistance in plants, whether their performance differs from dissolved Si species and which molecular pathways they may induce.

To fend off potential pathogens, plants have evolved disease resistance mechanisms that share mechanistic principles with the innate immunity of animals¹¹. An especially interesting form of plant disease resistance is the so-called induced resistance in which the disease resistance of the plant can be enhanced by previous exposure to beneficial rhizosphere microorganisms, avirulent and virulent pathogens, or specific resistance-inducing chemical compounds^{12–14}. A hallmark of induced resistance is its activity against a broad spectrum of pathogens. While the induction of plant disease resistance using chemical compounds is relatively well understood¹², the benefit of using slow nano-enabled delivery systems for the same purpose has not been investigated via systematic experiments^{1,7}.

A special form of induced resistance is systemic acquired resistance (SAR) that is characterized by the spread of locally induced

disease resistance to the whole plant^{15,16}. SAR is induced in all plant parts after locally challenging the plant with a pathogen or by the local application of so-called resistance-inducing compounds. Both these treatments induce signal transduction pathways that lead to the production of signals moving to distant tissues¹⁴. A key signalling compound that contributes to SAR is the plant hormone salicylic acid (SA) that is responsible for the activation of pathogenesis-related (PR) genes^{16,17}. Other factors include, for example, nitric oxide and reactive oxygen species^{18,19}. The fact that SAR can be activated by the application of resistance-inducing compounds^{12,13} makes SAR an attractive alternative strategy for controlling crop pests without the need for using irreversible genetic modifications or environmentally problematic pesticides.

SAR-inducing compounds such as benzothiadiazole successfully enhance disease resistance, but also reduce crop yields^{20,21}. Interestingly, Si-based compounds also seem to have the capacity to induce disease resistance via a broad range of different and partially still unknown mechanisms, including the mechanical reinforcement of defensive structures of the plant architecture, most notably the cell wall^{3,22}, but also the activation of biochemical defences^{3,23}. For example, biochemically, root-applied Si led to a broad-spectrum resistance against powdery mildew pathogen by increasing the activity of defence-related enzymes in leaves²⁴. It is important to note that the protective effect of Si seems to have—in contrast to other biostimulants such as benzothiadiazole—no negative effects on the growth and yield of plants^{3,25}. All this makes Si an attractive candidate to strengthen plant stress tolerance. Initial studies found that SiO_2 NPs may induce stress tolerance similar to conventional Si products, but a clear mechanistic understanding of the underlying processes is still lacking^{7,8,26,27}.

In this Article, we demonstrate the potential of SiO_2 NPs in inducing local and systemic disease resistance in the widely used model plant *Arabidopsis thaliana* against the bacterial pathogen *Pseudomonas syringae*. Silicic acid was assessed in parallel to disentangle the potential differences in the mode of action of dissolved

¹Department of Biology, University of Fribourg, Fribourg, Switzerland. ²Department of Botany and Microbiology, Faculty of Science, Tanta University, Tanta, Egypt. ³Adolphe Merkle Institute, University of Fribourg, Fribourg, Switzerland. ⁴Department of Chemistry, University of Fribourg, Fribourg, Switzerland.

✉e-mail: m.shetehy@uky.edu; fabienne.schwab@alumni.ethz.ch

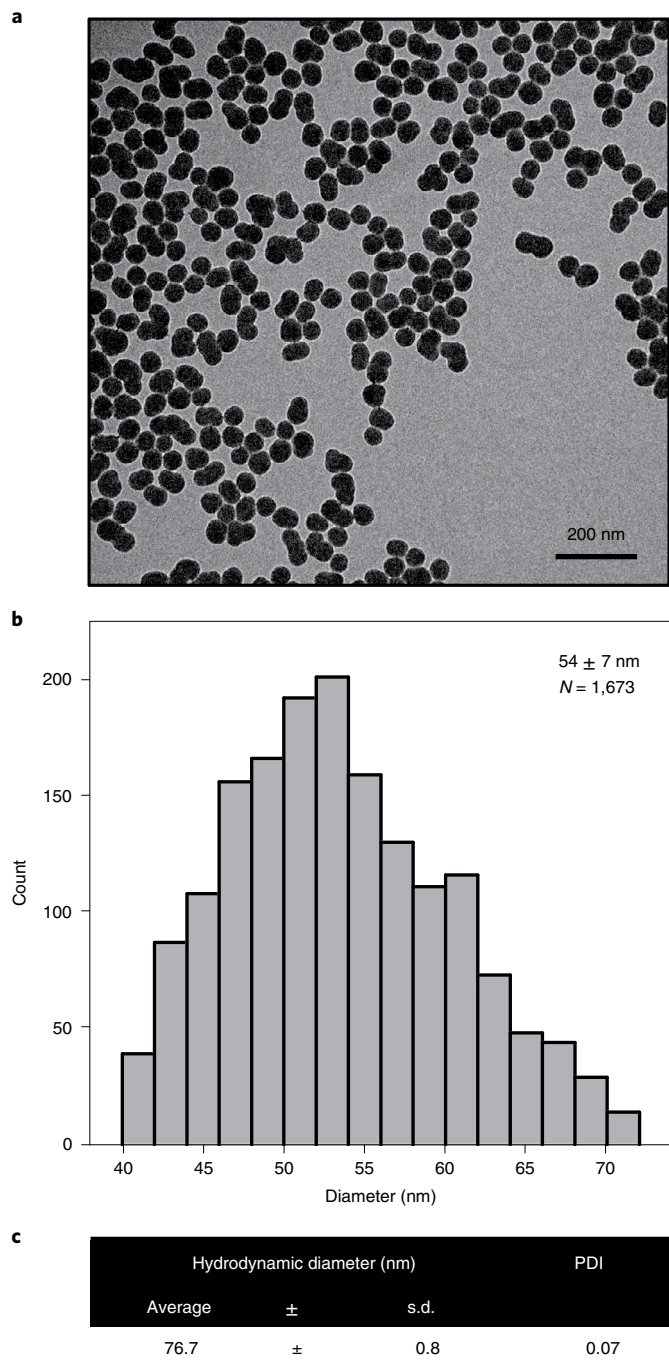


Fig. 1 | SiO₂ NPs under investigation. **a**, TEM image of the particles. **b**, Particle size distribution based on the TEM image analysis. **c**, DLS measurements of the SiO₂ NPs. The hydrodynamic radius is consistent with the primary particle size shown in **a** and **b**. PDI, polydispersity index. Averages \pm standard deviations. For the DLS measurements, number of measurements $N = 10$.

Si species compared with SiO₂ NPs. We assessed the role of SA and reactive-oxygen-species defence-related genes, established the therapeutic concentration range of SiO₂ NPs to induce the desired beneficial effects in plants, compared the laboratory setup (infiltration of selected leaves) with the more realistic spray application and visualized the nanoparticle–leaf interactions using transmission electron microscopy (TEM), with important implications for future strategies to apply nanoscale active ingredients for slow release in leaves.

SiO₂ NPs and subcellular distribution within the leaf. The SiO₂ NP suspensions used for the dosing of plants (Fig. 1) were well dispersed with a hydrodynamic particle size of 76.7 ± 0.8 nm (average \pm standard deviation) and a polydispersity index of 0.07. The primary particle size, as determined by TEM, was 54 ± 7 nm (average \pm standard deviation). The interaction of the nanoparticles with the plant was assessed by TEM (Fig. 2) 2 d after the application of SiO₂ NPs. Preliminary experiments showed that at this time point, the SiO₂ NP-exposed plants had already developed resistance. The size range of ~ 50 –70 nm of the nanoparticles allowed them to enter the leaf exclusively through the stomata and distribute within the large extracellular air spaces of the spongy mesophyll without penetrating any cell walls (Fig. 2 and Supplementary Fig. 1). The SiO₂ NPs remained within the air spaces of the leaf during the 2 d between their application and the time point of TEM observation. At the same time, the size of the nanoparticles prevented (undesirable) nanoparticle uptake into the cytoplasm as well as cell-to-cell translocation through the plasmodesmata (Fig. 2b). This is in line with previous studies in the literature based on the nanometre-resolution imaging of nanoparticles in plants, suggesting that the cutoff for root-shoot nanoparticle translocation is at approximately < 36 nm and it is < 15 –40 nm (basal size exclusion limits of ~ 3 –4 nm) for cell-to-cell plasmodesmata transport¹⁰. Compared with the fully closed stomata in the control plants (samples were kept in the dark for fixation), the nanoparticle-treated plants showed incompletely closed stomata as the nanoparticles were stuck in between the guard cells (Fig. 2b).

Exogenous application of SiO₂ NPs confers SAR. The local defence responses of *Arabidopsis* sprayed with SiO₂ NPs or a control treatment to virulent *P. syringae* were quantified via bacterial growth on leaves (Fig. 3a). Due to the lack of the *avrRpt2* gene in the virulent *P. syringae* that is needed by the Resistance to *Pseudomonas syringae* protein 2 (*RPS2*) resistance gene in *Arabidopsis* to induce a strong plant defence against *P. syringae*^{28,29}, a severe infection would be expected. However, a pronounced infection occurred only in the control treatment. Plants sprayed with SiO₂ NPs showed an eightfold improvement in basal resistance compared with the 4-(2-hydroxyethyl)-1-piperazineethanesulfonic acid (HEPES)-buffer-treated control plants (Fig. 3a), demonstrating that the SiO₂ NPs induced local defence in the plant within 24 h (the nanoparticles were applied 24 h before inoculation with the virulent *P. syringae*). The number of bacteria was reduced eightfold in SiO₂ NP-treated plants compared with the control.

The systemic responses of wild-type *Arabidopsis* plants to SiO₂ NPs and dissolved Si species are reflected in the inhibited bacterial growth, as shown in Fig. 3b,c. The positive control showed that plants previously infiltrated with the avirulent *P. syringae*, which is known to induce SAR, expectedly contained tenfold less virulent *P. syringae* compared with magnesium chloride (MgCl₂)- or HEPES-preinfiltrated plants (Fig. 3b,c). Remarkably, treating local leaves with SiO₂ NPs led to comparable systemic protection against virulent *P. syringae* as observed in the positive avirulent *P. syringae* control (Fig. 3a), which is equal to $> 90\%$ bacterial inhibition. It is highly unlikely that a local response to SiO₂ NPs or Si(OH)₄ in the distal tissue has caused this resistance because of the observed distribution and very slow dissolution of SiO₂ NPs (Fig. 2 and Supplementary Fig. 1) and the passive transport³⁰ and high reactivity of Si(OH)₄. This shows that treating *Arabidopsis* with SiO₂ NPs induced local and systemic resistance to *P. syringae*.

It is well known that Si(OH)₄ improves plant defences against different plant pathogens such as fungi, bacteria and viruses^{5,7}. We, therefore, also tested SAR in response to Si(OH)₄ (Fig. 3c) and found that treatment with Si(OH)₄ was able to induce SAR. These results suggest that Si(OH)₄ released from SiO₂ NPs is at least partially responsible for the SAR-inducing ability of SiO₂ NPs and that the SiO₂ NPs can act as a slow-release source for Si(OH)₄.

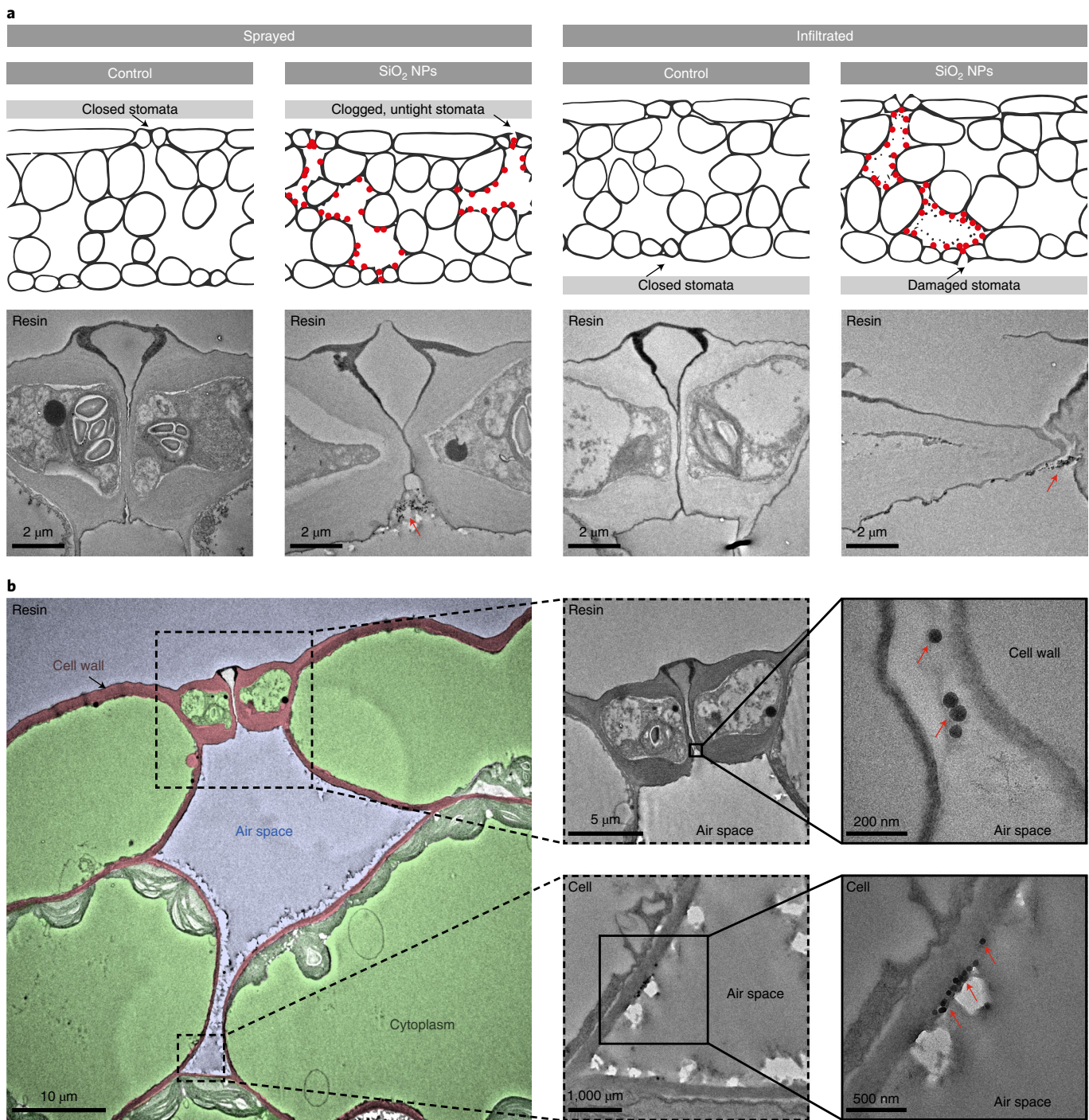


Fig. 2 | TEM of SiO_2 NP distribution and physiological effects in *Arabidopsis* leaves. Red arrows and dots, nanoparticles. Comparison between the spray application used in the field and for local defence assays and the infiltration application used in laboratory studies. Images obtained when the plants had already developed resistance 2 d after exposure to SiO_2 NPs. **a**, Control leaves only treated with the buffer solution. **b**, TEM overview image and zoomed-in views of the stoma and cell-air space interface. False colours: red, cell wall (apoplast); green, cytoplasm (symplast); blue, spaces filled with air. SiO_2 NP-sprayed leaf at a higher resolution shows that the stomata are not tightly closed anymore due to nanoparticle uptake and clogging. Nanoparticles entered through the stomata into the air spaces of the leaf, and they were also found to be extracellularly adsorbed on the outer edge of the cell walls in the air gaps of the spongy mesophyll; they were absent in the cytoplasm (intracellular space). Higher-resolution TEM image is shown in Supplementary Fig. 1.

Measuring the exact amount of free $\text{Si}(\text{OH})_4$ directly in Plantae is challenging due to the low concentrations and fragile equilibrium of the dissolved $\text{Si}(\text{OH})_4$ and Si oligomers and the solid SiO_2 species^{2,4,31} (Supplementary Information, ‘Details on $\text{Si}(\text{OH})_4$ analytics’). We, therefore, resorted to direct TEM imaging of the nanoparticles

in the plants; at high resolution, abundant intact SiO_2 NPs were observed in the stomata 2 d after the SiO_2 NP treatments (Fig. 2). This demonstrates that the plants could not degrade the nanoparticles at the time point of inoculation with virulent *P. syringae* (in all the assays, the nanoparticles were applied at least 24 h before

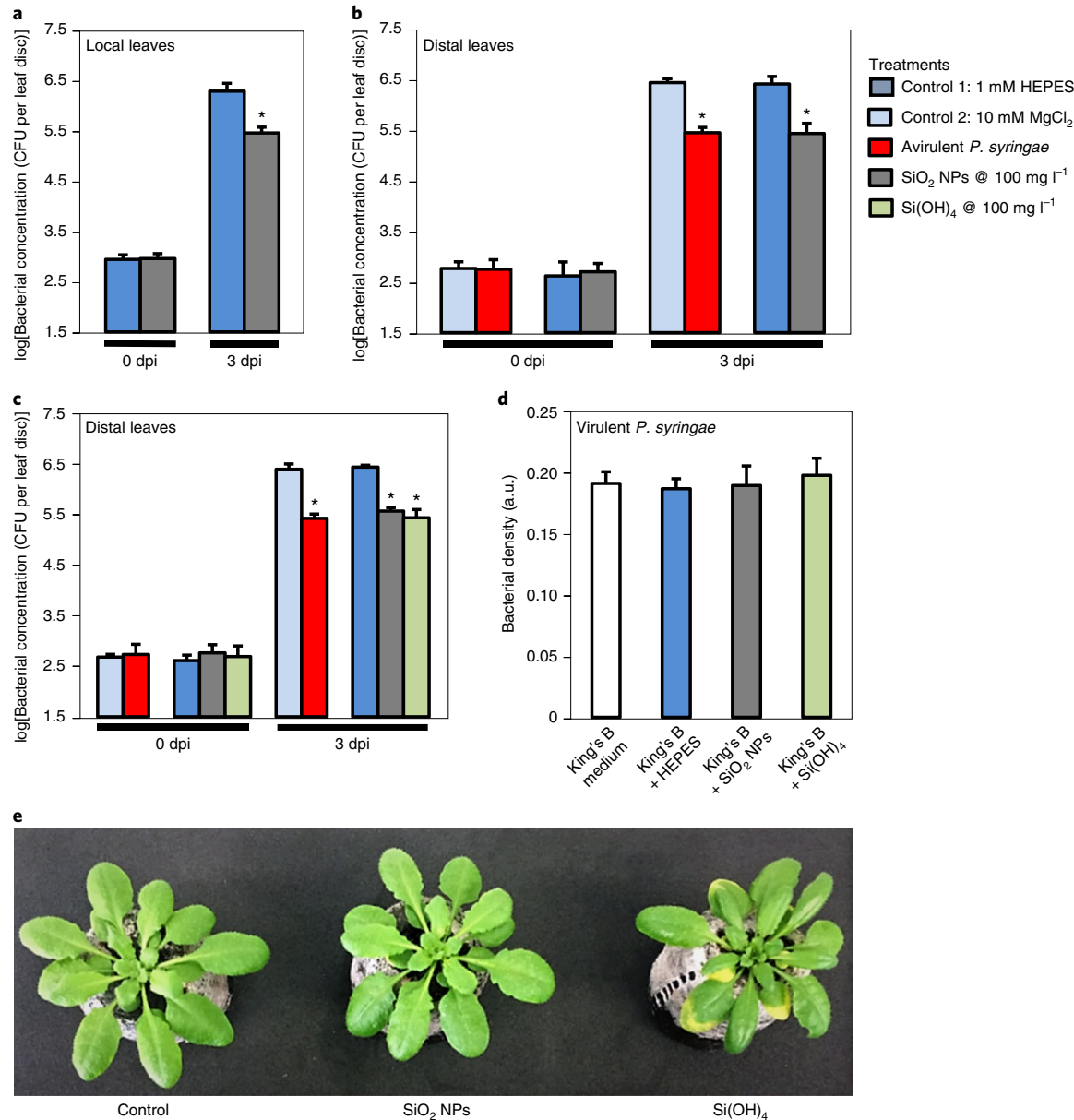


Fig. 3 | Enhanced local and systemic disease resistance in wild-type Col-O *Arabidopsis* to *P. syringae* induced by SiO₂ NPs or Si(OH)₄. The bacteria in the leaves were quantified 0 and 3 dpi. **a**, Growth of virulent *P. syringae* in leaves. The plants were sprayed with different treatments, and virulent *P. syringae* was inoculated 24 h later. **b**, SAR in distal leaves. Plants locally infiltrated with different treatments. 48 h later, virulent *P. syringae* was inoculated on untreated systemic leaves. **c**, SAR in distal leaves; repetition of the experimental setup in **b** with an additional Si(OH)₄ treatment. **d**, No effect of SiO₂ NPs and Si(OH)₄ on the in vitro growth of virulent *P. syringae* bacteria in the absence of the plant. **e**, Phenotype of the *Arabidopsis* plants. Plants pretreated with the HEPES buffer (control), SiO₂ NPs or Si(OH)₄ (1,000 mg SiO₂ l⁻¹ each). Note that the yellow leaves in the plant exposed to Si(OH)₄ coincide with the upregulated expression of the oxidative stress marker gene shown in Fig. 4c. In **a-d**, all the experiments were performed twice with comparable results. Bars and whiskers are averages and standard deviations; *N*=3; one-way analysis of variance (ANOVA); post hoc least significant difference; *P*<0.01.

inoculation). The slow nanoparticle dissolution is in line with the slow dissolution kinetics of the SiO₂ NPs measured previously in water (half-life of ~66 d at pH 7)³².

To test whether SiO₂ NPs and Si(OH)₄ have a direct toxic effect on bacterial growth, virulent *P. syringae* was cultivated in vitro in the presence or absence of SiO₂ NPs or Si(OH)₄ at the lowest fully effective dose of SiO₂ NPs at 100 mg l⁻¹. At these concentrations that induced strong defence in plants, neither SiO₂ NPs nor Si(OH)₄ alone harmed the growth of the virulent *P. syringae* bacteria (Fig. 3d), demonstrating that SiO₂ NPs induce resistance in plants

by activating the defence responses in plants and not by directly inhibiting the bacterial growth.

Dose dependence of SAR response. The SAR was further tested in response to different concentrations of SiO₂ NPs or Si(OH)₄; for additional validation, a second bacterial growth quantification method³³ based on bacterial DNA was used (Fig. 4a,b and Supplementary Table 1). Treatment with SiO₂ NPs at a concentration of 25 mg SiO₂ l⁻¹ already resulted in a partial reduction of 29% of bacterial growth in systemic leaves, and treatment with 100 mg ml⁻¹

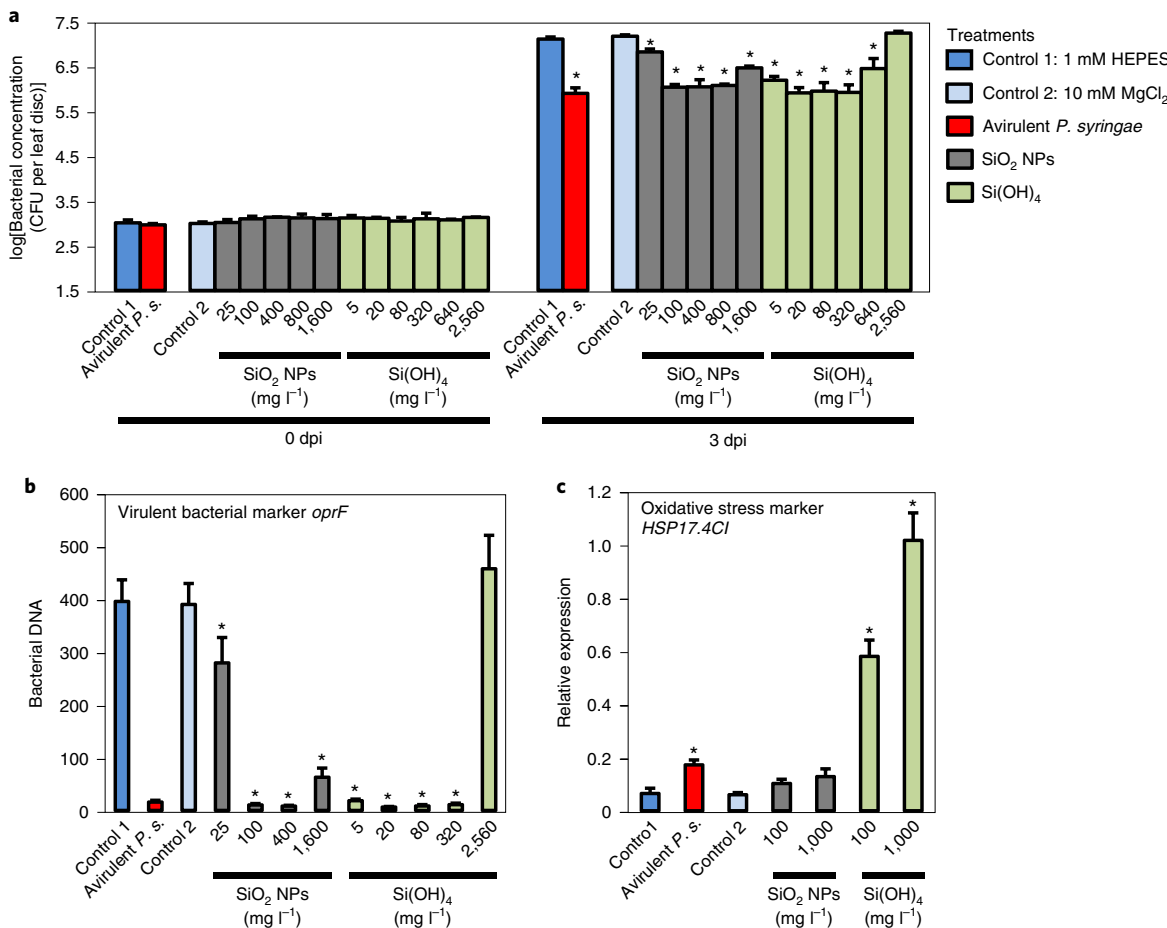


Fig. 4 | SiO₂ NPs confer SAR in a dose-dependent manner. Distal leaves of wild-type Col-0 *Arabidopsis* treated with the control, SiO₂ NPs or Si(OH)₄.

a, SAR in plants locally infiltrated with different treatments. After 48 h, virulent *P. syringae* was inoculated on untreated systemic leaves. The bacteria in the leaves were quantified 0 and 3 dpi. **b**, qPCR transcript levels of *oprF* gene from virulent *P. syringae* using DNA templates extracted from the inoculated leaves. **c**, RT-qPCR transcript levels of the oxidative stress marker gene *AtHSP17.4C1* in response to different treatments. Plants were locally infiltrated with different treatments. Leaves sampled 48 h after treatments. Reference gene, At4g26410 (*expG*). Bars and whiskers are averages and standard deviations; *N*=3; one-way ANOVA; post hoc least significant difference; *P*<0.05. All the experiments in **a–c** were performed twice with comparable results.

resulted in maximum protection (>90%) compared with the positive control plants preinfiltrated with avirulent *P. syringae* (Fig. 4a). As the series of concentrations shown in Fig. 4a, higher concentrations of SiO₂ NPs exceeding 1,600 mg SiO₂ l⁻¹ led to increased bacterial infection and were thus less effective in activating SAR. Pretreatment with a concentration of 5 mg SiO₂ l⁻¹ of Si(OH)₄ (concentration normalized to SiO₂ l⁻¹ for the sake of comparability) led to a reduction of 81% in the bacterial numbers compared with the positive control. Maximum protection with a reduction similar to the control plants preinfiltrated with avirulent *P. syringae* was achieved at concentrations between 20 and 320 mg SiO₂ l⁻¹. A higher concentration of 640 mg SiO₂ l⁻¹ was less effective, and a concentration of 2,560 mg SiO₂ l⁻¹ was ineffective in inducing SAR, demonstrating a detrimental effect of higher concentrations of Si(OH)₄ on SAR induction.

The data in Fig. 4 served to establish a dose-response relationship between SAR and the SiO₂ NP concentration (Fig. 5a). Using a standard log-logistic dose-response model, the dynamic range and the effective concentration at 50% bacterial inhibition (EC50) was determined as 0.4 ± 0.04 mM Si (average \pm standard deviation) for SiO₂ NPs (that is, 24 mg SiO₂ l⁻¹; Supplementary Fig. 2 shows the residual analysis and Supplementary Table 2 lists the fitting parameters) in a range of 25–100 mg SiO₂ l⁻¹. For spraying, the EC50 may

be similar to the injected SiO₂ NPs, as both the local (sprayed) and the systemic (injected) assays at 100 mg SiO₂ l⁻¹ resulted in disease resistance (Fig. 3 and Fig. 6a,b).

The results based on counting bacterial colonies were confirmed by estimating the bacterial biomass based on a quantitative PCR (qPCR) analysis of the bacterial outer membrane protein gene *oprF* (Fig. 4b). The bacterial DNA levels were in good agreement with the bacterial colony counting results shown in Fig. 4a, which is in line with a previous research that compared the two techniques³³.

In contrast to SiO₂ NPs, higher concentrations of Si(OH)₄ adversely affected the phenotype of the treated plants (Fig. 3e). At a concentration of 1,000 mg SiO₂ l⁻¹, the leaves of the plants treated with Si(OH)₄ showed signs of chlorosis (yellowing), whereas the leaves of the plants treated with SiO₂ NPs looked healthy (Fig. 3e). This different behaviour at higher concentrations prompted us to further investigate the negative effect of higher concentrations of SiO₂ NPs and Si(OH)₄. The expression level of the heat shock protein *AtHSP17.4C1*, a molecular marker for oxidative stress³⁴, was analysed by qPCR with reverse transcription (RT-qPCR). The *HSP17.4C1* transcript levels were determined in response to avirulent *P. syringae*, SiO₂ NPs or Si(OH)₄ (100 and 1,000 mg SiO₂ l⁻¹; Fig. 4c) 2 d after the treatments. Treatment with avirulent *P. syringae* caused a minor increase (2.7-fold) in the *AtHSP17.4C1* expression

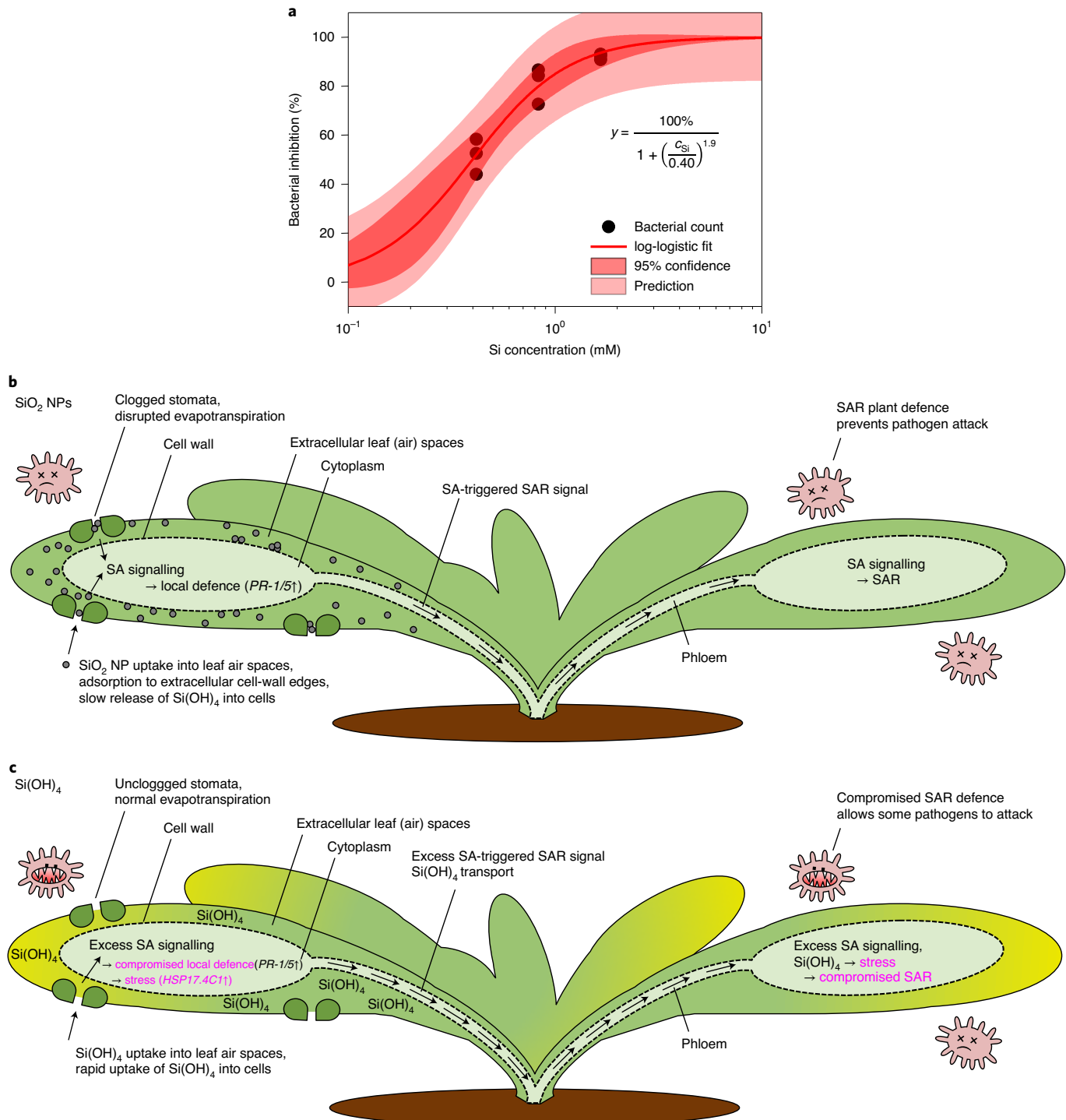


Fig. 5 | Dynamic range for SAR induced in distal leaves by SiO_2 NPs in *A. thaliana*, and model summarizing the observed plant-defence-enhancing actions of SiO_2 NPs and $\text{Si}(\text{OH})_4$. **a**, Data from Fig. 4a. SiO_2 NP-triggered dose-dependent bacterial inhibition 3 d after infection of wild-type *A. thaliana* with virulent *P. syringae*. The EC₅₀ value was 0.40 ± 0.04 mM Si (average \pm standard deviation) for SiO_2 NPs (that is, $24 \text{ mg SiO}_2 \text{ l}^{-1}$). Above the dynamic range, the bacterial infection can increase again (Fig. 4a). Six data points at 0 mM Si are not shown due to the nature of the log axis, but they are apparent in the detailed residual analysis shown in Supplementary Fig. 2 and Supplementary Table 2. C_{Si} , Si concentration in mM. **b**, SiO_2 NPs act by (1) slowly releasing $\text{Si}(\text{OH})_4$ into cells, triggering SA, and thus local defence and SAR; (2) clogging stomata, triggering SA and subsequent defences. Absence of intracellular nanoparticles confirmed by electron microscopy (Fig. 2 and Supplementary Fig. 1). **c**, $\text{Si}(\text{OH})_4$ instantly diffuses into cells, triggering SA and subsequent local defence and SAR. However, the instant uptake causes overdose, stress and compromised defences. Both the mechanisms are shown after treatment with the same amount of SiO_2 equivalents ($1,000 \text{ mg SiO}_2 \text{ l}^{-1}$). SA, plant hormone regulating SAR and *PR-1/5* gene expression; *PR-1/5*, genes encoding PR proteins 1 and 5; *HSP17.4C1*, heat shock protein and oxidative stress marker gene.

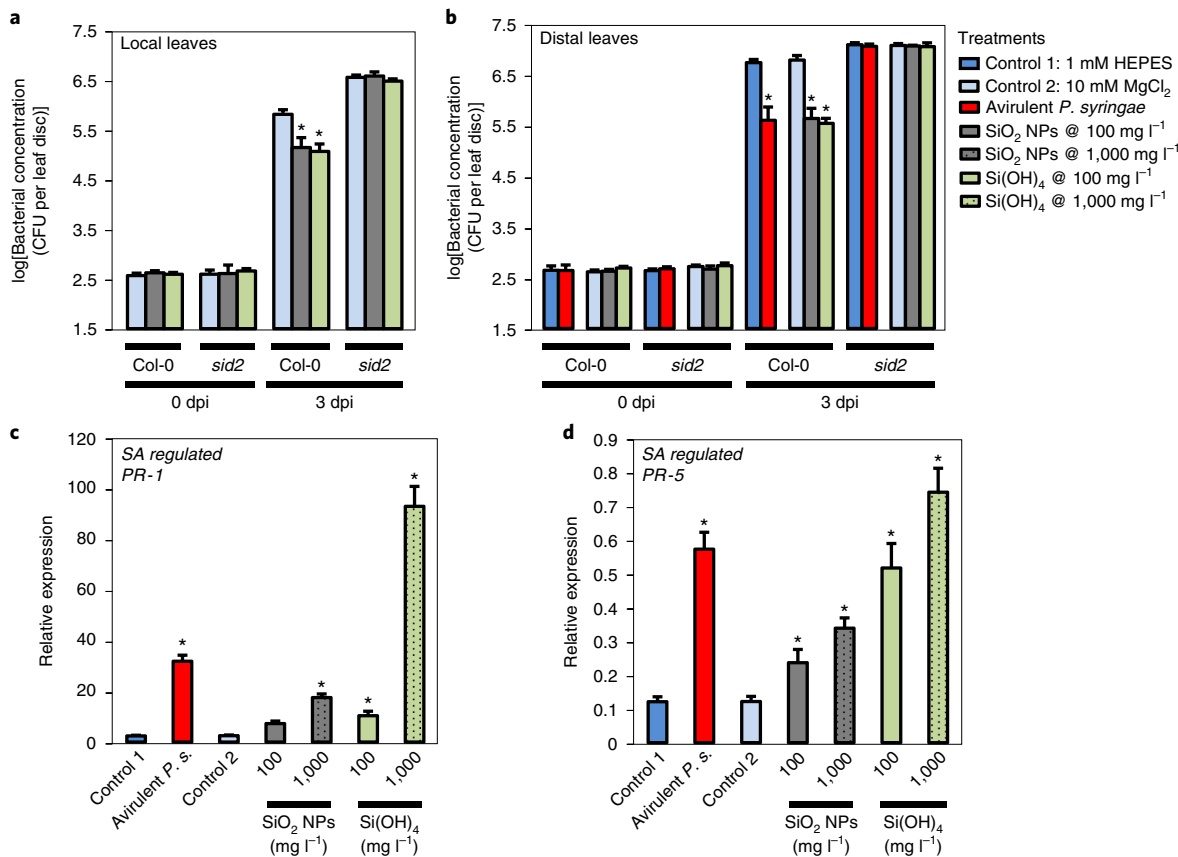


Fig. 6 | SiO₂ NPs induce disease resistance based on SA-dependent pathway. Experiments in *Arabidopsis* wild-type Col-0 and sid2. The bacteria in the leaves were quantified 0 and 3 dpi. **a**, *A. thaliana* wild-type Col-0 and sid2 were locally infiltrated with different treatments. After 24 h of these treatments, virulent *P. syringae* was inoculated. **b**, SAR in the distal leaves of wild-type Col-0 and mutant sid2. Plants were locally infiltrated with different treatments. After 48 h of these treatments, virulent *P. syringae* was inoculated. **c,d**, RT-qPCR analysis of the gene expression of the SA-regulated genes AtPR-1 (**c**) and AtPR-5 (**d**) in response to different local treatments of wild-type *Arabidopsis*. Leaves sampled 48 h after treatments. Reference gene, At4g26410 (expG). Bars and whiskers are averages and standard deviations; *N*=3; one-way ANOVA; post hoc least significant difference; *P*<0.02. All the experiments in **a-d** were performed twice with comparable results.

compared with the control. Similarly, treatment with SiO₂ NPs led to a 1.6-fold (100 mg SiO₂ l⁻¹) and twofold (1,000 mg SiO₂ l⁻¹) increase in transcript abundance relative to the control treatment that was not statistically significant. However, treatment with higher concentrations of Si(OH)₄ caused stress, as the transcript levels of the oxidative stress marker gene HSP17.4C1 were induced ninefold at a concentration of 100 mg SiO₂ l⁻¹ and 18-fold at 1,000 mg SiO₂ l⁻¹.

SiO₂ NP-mediated SAR depends on SA. The plant hormone SA plays a core regulatory role in plant immunity³⁵. Thus, we tested the ability of SiO₂ NPs to induce local disease resistance and SAR in an *Arabidopsis* mutant defective in SA biosynthesis (SA induction-deficient 2 (sid2)³⁶) to check if SiO₂ NPs confer SAR via SA-dependent defence pathway or not. Notably, neither Si(OH)₄ nor SiO₂ NPs induced local disease resistance or SAR in sid2 mutant plants, while they induced basal disease resistance and SAR in wild-type plants (Fig. 6a,b), demonstrating that SA-dependent defence signalling is essential for Si(OH)₄- and SiO₂ NP-induced disease resistance. To further support this result, we next quantified the expression of the SA-responsive marker genes PR protein 1 (*PR-1*, gene *AtPR-1*) and *PR-5* (gene *AtPR-5*) in wild-type plants (Fig. 6c,d). Similar to treatment with avirulent *P. syringae*, treatment with Si(OH)₄ and SiO₂ NPs resulted in an up to 30-fold and 6-fold increase in the transcript abundance of *AtPR-1* (Fig. 6c) and *AtPR-5* (Fig. 6d), respectively, compared with the control

treatments. Hence, both Si(OH)₄ and SiO₂ NPs activated SA-dependent defence reactions. Although SiO₂ NPs triggered lower *AtPR-1* and *AtPR-5* expression levels in comparison with avirulent *P. syringae*-infiltrated plants and Si(OH)₄-treated plants, the inducing effect was sufficient to confer SAR.

Implications on the mode of action of leaf-applied SiO₂ NPs. The pathosystem involving *Arabidopsis* and the hemibiotrophic bacterial pathogen *P. syringae* offers an ideal model to investigate the effect of SiO₂ NPs and Si(OH)₄ on plant defence. Our results (summarized in the model in Fig. 5b,c) show that the protective effect of SiO₂ NPs and Si(OH)₄ is based on the ability to induce basal resistance and SAR (Fig. 3a-c) and not on the direct toxic effects as neither SiO₂ NPs nor Si(OH)₄ inhibited bacterial growth (Fig. 3d). Our data are in line with the initial results that suggested that Si(OH)₄ and sometimes SiO₂ NPs can protect plants from different plant pathogens^{7,26,27,37}; nevertheless, here we show that the mechanism had no toxic effect on the pathogen, but rather induced the defences of the plant.

Both SiO₂ NPs and Si(OH)₄ induce SAR in a dose-dependent manner, leading to bacterial inhibition of >90% compared with the control plants treated only with the HEPES buffer or MgCl₂. These results are consistent with the previous results suggesting that SiO₂ NPs and Si(OH)₄ function in a dose-dependent manner in plants and animals^{26,27,38}. However, instead of the previously proposed

pesticidal action of SiO_2 NPs, we show here that the nanoparticles caused an increase in the plant defence. Our data suggest that the SiO_2 NPs used in the present study can be successfully used to slowly release $\text{Si}(\text{OH})_4$ to the plant from within the spongy mesophyll (Fig. 2) in close direct interaction with the diffusion layer on the plant cell walls, which is at least partially responsible for the SAR-inducing ability of SiO_2 NPs. Water (vapour) secreted from the plant cell wall or the plant-induced dissolution of SiO_2 NPs linked to increased secretory activity¹⁰ (exudates) may have promoted the further dissolution of $\text{Si}(\text{OH})_4$. Based on the release rates of SiO_2 NPs that were determined earlier under conditions optimized for dissolution in a continuously depleted ultrapure water system (half-life of ~66 d at pH 7)³², a maximum of ~13% particles could have dissolved within 48 h of SiO_2 NP exposure. Si-containing reaction byproducts of the nanoparticle synthesis were ruled out to play a notable role in the induction of defence (Supplementary Information, 'Si reaction byproducts'). The maximum released $\text{Si}(\text{OH})_4$ from SiO_2 NPs could, therefore, explain the bacterial inhibition; however, it cannot fully explain the lack of oxidative stress responses and higher bacterial DNA levels for SiO_2 NPs in the plants (Fig. 4b). Probably, the absence of peak $\text{Si}(\text{OH})_4$ concentrations resulted in lower $\text{Si}(\text{OH})_4$ toxicity for both bacteria and plants. Other effects such as modulated evapotranspiration due to the blockage and incomplete closure of the stomata by the nanoparticles (Fig. 2), which can cause SA-related responses similar to drought stress³⁹, and the close interaction of the nanoparticles with cells in the spongy mesophyll may play an important role; this is in line with earlier research about stomata as ports of entry for pollutants and nanoparticles^{40,41}. The exact relative contribution of each effect remains to be elucidated in follow-up studies. It is important to note that the cell walls in the mesophyll air spaces have very thin, or lack, cuticular waxes¹⁰, and therefore, it is in contrast to the external leaf surface; a direct interaction of the nanoparticles can take place with the cell wall and thus the apoplast transport system including the xylem. Irrespective of the detailed mechanism of the nanoparticles, this is of importance for any nanoagrochemical application aiming at the slow release of active ingredients, because nanoparticles in the extracellular spongy mesophyll air spaces (Fig. 2 and Supplementary Fig. 1) can interact with the leaf for extended periods without being washed away by rain.

High concentrations of $\text{Si}(\text{OH})_4$ caused the chlorosis of leaves indicative of stress (Fig. 3e). An increased expression of the oxidative stress marker gene *AtHSP17.4C1* (ref. ³⁴) confirmed stress in the $\text{Si}(\text{OH})_4$ treatment at 100 and 1,000 mg $\text{SiO}_2\text{l}^{-1}$, as the transcript levels of *AtHSP17.4C1* were more strongly induced compared with avirulent *P. syringae* or SiO_2 NP treatments (Fig. 4c). Together, these data show that $\text{Si}(\text{OH})_4$ was more toxic to plants than SiO_2 NPs. Hence, impaired SAR in plants treated with higher concentrations of $\text{Si}(\text{OH})_4$ (Fig. 4a) might be linked to enhanced oxidative stress, consistent with the fact that higher levels of nitric oxide and reactive oxygen species were shown to impair the induction of SAR^{19,23}. For SiO_2 NPs, no substantial increase in the oxidative stress marker gene was found (Fig. 4c). Impaired SAR for SiO_2 NPs occurred only at very high concentrations in the gram per litre range (Fig. 4a), probably due to the excess release of $\text{Si}(\text{OH})_4$ causing oxidative stress or the highly intense clogging of the stomata (Fig. 2) that disrupted evapotranspiration. While the low polydispersity index measured by dynamic light scattering (DLS) (Fig. 1c) indicates well-dispersed SiO_2 NP suspensions even at higher concentrations, heteroaggregation with mucilage in the stomata (upon contact with the leaf) and probably homoaggregation (at higher nanoparticle concentrations) appeared to promote the clogging of the stomata (Fig. 2a, red arrows). These results are in line with ref. ⁸, according to which SiO_2 NP concentrations up to 1,000 mg $\text{SiO}_2\text{l}^{-1}$ were not phytotoxic despite the uptake of SiO_2 NPs into the root system of *A. thaliana*. Our results are also consistent with the initial studies^{42,43} that found

better effects of SiO_2 NPs on plant growth than conventional silica fertilizers. In conclusion, the application of SiO_2 NPs can reduce the risk of overdosage.

Our data demonstrate that SiO_2 NPs- and $\text{Si}(\text{OH})_4$ -mediated SAR acts via the activation of the SA-dependent defence pathway, which is a key component of the basal disease resistance and SAR^{44,45}. Neither SiO_2 NPs nor $\text{Si}(\text{OH})_4$ induced resistance in *sid2* that has a defect in the SA biosynthesis (Fig. 6a,b). The induction of resistance by SiO_2 NPs was comparable to the effect of $\text{Si}(\text{OH})_4$ at intermediate concentrations, although the soluble fraction of $\text{Si}(\text{OH})_4$ in this treatment was far lower as the particles dissolved only partially in the plant, if at all (Fig. 2), suggesting that SiO_2 NPs can induce SA-dependent defence pathways as intact particles. Furthermore, the expression levels of two SA-responsive marker genes, namely, *AtPR-1* and *AtPR-5* encoding *PR-1* and *PR-5*, respectively, were induced in response to SiO_2 NPs and $\text{Si}(\text{OH})_4$ (Fig. 6c,d). These results are in line with ref. ⁴⁶, who reported that the exogenous application of $\text{Si}(\text{OH})_4$ induced SA biosynthesis in leaves exposed to the fungal pathogen *Erysiphe cichoracearum*. In addition, Si-primed tomato plants were protected against *Ralstonia solanacearum* via the upregulation of SA-controlled defence gene expression⁴⁷. Although SiO_2 NPs triggered lower *AtPR-1* and *AtPR-5* expression levels than the plants infiltrated with avirulent *P. syringae* and $\text{Si}(\text{OH})_4$ -treated plants, the achieved level of expression was sufficient to confer a full SAR response.

Conclusions

The present results show that low concentrations of SiO_2 NPs efficiently protect the widely used model plant *Arabidopsis* from infection by the bacterial pathogen *Pseudomonas*, and they revealed the mode of action of SiO_2 NPs compared with the dissolved counterpart, $\text{Si}(\text{OH})_4$. The protective effect of SiO_2 NPs is mediated by the activation of SA-dependent plant immunity responses and is partially based on the slow release of $\text{Si}(\text{OH})_4$ from nanoparticles entering through the stomata and distribution within the spongy mesophyll and probably partially by intact nanoparticle-induced SA-dependent responses.

Compared with direct $\text{Si}(\text{OH})_4$ application, SiO_2 NPs proved to be safer for the plant. They did not cause phytotoxicity even at concentrations tenfold higher than the minimal dose needed for plant protection and therefore have a broader therapeutic range than $\text{Si}(\text{OH})_4$. The lowest fully effective dose (100 $\text{SiO}_2\text{l}^{-1}$) is promising because it corresponds to an extrapolated field dose of only 3 kg $\text{SiO}_2\text{ha}^{-1}$, corresponding to more than 1,000-fold material savings compared with the solid bulk SiO_2 treatments. This calculation assumes a typical 300 lha^{-1} application (conventional aqueous spray volumes for pesticide application equipment⁴⁸), and an uncertainty factor of 100 for the concentration. Contrary to previous assumptions about the ability of nanoparticles to penetrate the cuticle, SiO_2 NP intake was clearly restricted to the stomata and the extracellular spongy mesophyll, confirming our hypothesis that the leaf cuticle represents an impermeable barrier to nanoparticles¹⁰, which is in line with earlier fundamental research⁴⁹. The spongy mesophyll is an attractive target for the long-term deposition of slow-release nanoagrochemicals. Future research should extend the investigations to a broader spectrum of defence-related genes with other plant pathogens and the biomechanical quantification of the physical effects of nanoparticles that affect leaf permeability and may trigger the SA-related responses. To further advance SiO_2 NPs as nanobiostimulants and fertilizers, which should be the case with every material or organism used in agriculture, the long-term effects of SiO_2 NPs to occupationally exposed agricultural workers and non-target organisms, such as beneficial soil microorganisms or bees, must be thoroughly analysed before broad commercial application. The potential risks of nanoagrochemicals and possible strategies for risk mitigation have been thoroughly reviewed

previously^{1,50,51}. Amorphous SiO₂ NPs have already been approved by the Food and Drug Administration as they are generally regarded as safe, and they are in use as dietary additives (E551)⁵² in a broad range of foodstuffs such as table salt. The daily intake of nanoscale silica from food is estimated to be 1.8 mg kg⁻¹ (ref. ⁵³). Our own initial experiments with *Caenorhabditis elegans* nematodes used as model non-target microorganisms (Supplementary Fig. 3) have shown an ~36-fold lower ecotoxicity of SiO₂ NPs compared with liquid Si(OH)₄ preparations that are in use for plant nutrition since decades. Thus, compared with currently used treatments, the present SiO₂ NPs alone, or in combination with other active ingredients, promise to offer a cost-effective, consumer-safe strategy that is tracelessly degradable and a sustainable alternative to protect plants against pathogens via the controlled induction of SAR, without any negative effects on yield or non-target organisms associated with the action of previously described plant biostimulants or pesticides.

Online content

Any methods, additional references, Nature Research reporting summaries, source data, extended data, supplementary information, acknowledgements, peer review information; details of author contributions and competing interests; and statements of data and code availability are available at <https://doi.org/10.1038/s41565-020-00812-0>.

Received: 10 March 2020; Accepted: 30 October 2020;

Published online: 14 December 2020

References

- White, J. C. & Gardea-Torresdey, J. Achieving food security through the very small. *Nat. Nanotechnol.* **13**, 627–629 (2018).
- Casey, W., Kinrade, S., Knight, C., Rains, D. & Epstein, E. Aqueous silicate complexes in wheat, *Triticum aestivum* L. *Plant Cell Environ.* **27**, 51–54 (2004).
- Ma, J. F. & Yamaji, N. Silicon uptake and accumulation in higher plants. *Trends Plant Sci.* **11**, 392–397 (2006).
- Choplin, G. R., Pathak, P. & Thakur, P. Polymerization and complexation behavior of silicic acid: a review. *Main Group Met. Chem.* **31**, 53–72 (2008).
- Bélanger, R. R., Bowen, P. A., Ehret, D. L. & Menzies, J. G. Soluble silicon—its role in crop and disease management of greenhouse crops. *Plant Dis.* **79**, 329–336 (1995).
- Abdel-Halim, M. E., Hegazy, H. S., Hassan, N. S. & Naguib, D. M. Effect of silica ions and nano silica on rice plants under salinity stress. *Ecol. Eng.* **99**, 282–289 (2017).
- Luyckx, M., Hausman, J.-F., Lutts, S. & Guerriero, G. Silicon and plants: current knowledge and technological perspectives. *Front. Plant Sci.* **8**, 411 (2017).
- Slomberg, D. L. & Schoenfisch, M. H. Silica nanoparticle phytotoxicity to *Arabidopsis thaliana*. *Environ. Sci. Technol.* **46**, 10247–10254 (2012).
- Eichert, T., Kurtz, A., Steiner, U. & Goldbach, H. E. Size exclusion limits and lateral heterogeneity of the stomatal foliar uptake pathway for aqueous solutes and water-suspended nanoparticles. *Physiol. Plant.* **134**, 151–160 (2008).
- Schwab, F. et al. Barriers, pathways and processes for uptake, translocation and accumulation of nanomaterials in plants—critical review. *Nanotoxicology* **10**, 257–278 (2016).
- Jones, J. D. & Dangl, J. L. The plant immune system. *Nature* **444**, 323–329 (2006).
- Conrath, U. et al. Priming: getting ready for battle. *Mol. Plant Microbe Interact.* **19**, 1062–1071 (2006).
- Mauch-Mani, B., Baccelli, I., Luna, E. & Flors, V. Defense priming: an adaptive part of induced resistance. *Annu. Rev. Plant Biol.* **68**, 485–512 (2017).
- Ryals, J. A. et al. Systemic acquired resistance. *Plant Cell* **8**, 1809–1819 (1996).
- Ross, A. F. Systemic acquired resistance induced by localized virus infections in plants. *Virology* **14**, 340–358 (1961).
- Durrant, W. E. & Dong, X. Systemic acquired resistance. *Annu. Rev. Phytopathol.* **42**, 185–209 (2004).
- Mauch, F. et al. Manipulation of salicylate content in *Arabidopsis thaliana* by the expression of an engineered bacterial salicylate synthase. *Plant J.* **25**, 67–77 (2001).
- Wang, C. et al. Free radicals mediate systemic acquired resistance. *Cell Rep.* **7**, 348–355 (2014).
- El-Shetehy, M. et al. Nitric oxide and reactive oxygen species are required for systemic acquired resistance in plants. *Plant Signal. Behav.* **10**, e998544 (2015).
- Louws, F. et al. Field control of bacterial spot and bacterial speck of tomato using a plant activator. *Plant Dis.* **85**, 481–488 (2001).
- Romero, A., Kousik, C. & Ritchie, D. Resistance to bacterial spot in bell pepper induced by acibenzolar-S-methyl. *Plant Dis.* **85**, 189–194 (2001).
- Kim, S. G., Kim, K. W., Park, E. W. & Choi, D. Silicon-induced cell wall fortification of rice leaves: a possible cellular mechanism of enhanced host resistance to blast. *Phytopathology* **92**, 1095–1103 (2002).
- Wang, M. et al. Role of silicon on plant-pathogen interactions. *Front. Plant Sci.* **8**, 701 (2017).
- Liang, Y., Si, J. & Römhild, V. Silicon uptake and transport is an active process in *Cucumis sativus*. *New Phytol.* **167**, 797–804 (2005).
- van Bockhaven, J. et al. Silicon induces resistance to the brown spot fungus *Cochliobolus miyabeanus* by preventing the pathogen from hijacking the rice ethylene pathway. *New Phytol.* **206**, 761–773 (2015).
- Rouhani, M., Samih, M. & Kalantar, S. Insecticidal effect of silica and silver nanoparticles on the cowpea seed beetle, *Callosobruchus maculatus* F.(Col.: Bruchidae). *J. Entomol. Res.* **4**, 297–305 (2013).
- El-Helaly, A., El-Bendary, H., Abdel-Wahab, A., El-Sheikh, M. & Elnagar, S. The silica-nano particles treatment of squash foliage and survival and development of *Spodoptera littoralis* (Bosid.) larvae. *J. Entomol. Zool.* **4**, 175–180 (2016).
- Kunkel, B. N., Bent, A. F., Dahlbeck, D., Innes, R. W. & Staskawicz, B. J. *RPS2*, an *Arabidopsis* disease resistance locus specifying recognition of *Pseudomonas syringae* strains expressing the avirulence gene *avrRpt2*. *Plant Cell* **5**, 865–875 (1993).
- Chen, Z., Kloek, A. P., Boch, J., Katagiri, F. & Kunkel, B. N. The *Pseudomonas syringae* *avrRpt2* gene product promotes pathogen virulence from inside plant cells. *Mol. Plant Microbe Interact.* **13**, 1312–1321 (2000).
- Exley, C. A possible mechanism of biological silicification in plants. *Front. Plant Sci.* **6**, 853 (2015).
- Bossert, D. et al. A hydrofluoric acid-free method to dissolve and quantify silica nanoparticles in aqueous and solid matrices. *Sci. Rep.* **9**, 7938 (2019).
- Schwab, F. & Maceroni, M. A controlled release silica-based nanoparticle composition, method of production and fertilization methods. Patent WO2020212526A1 (2020).
- Ross, A. & Somssich, I. E. A DNA-based real-time PCR assay for robust growth quantification of the bacterial pathogen *Pseudomonas syringae* on *Arabidopsis thaliana*. *Plant Methods* **12**, 48 (2016).
- Sewelam, N., Kazan, K., Hüdig, M., Maurino, V. G. & Schenk, P. M. The *AtHSP17.4C1* gene expression is mediated by diverse signals that link biotic and abiotic stress factors with ROS and can be a useful molecular marker for oxidative stress. *Int. J. Mol. Sci.* **20**, 3201 (2019).
- An, C. & Mou, Z. Salicylic acid and its function in plant immunity. *J. Integr. Plant Biol.* **53**, 412–428 (2011).
- Nawrath, C. & Métraux, J.-P. Salicylic acid induction-deficient mutants of *Arabidopsis* express *PR-2* and *PR-5* and accumulate high levels of camalexin after pathogen inoculation. *Plant Cell* **11**, 1393–1404 (1999).
- Ye, M. et al. Priming of jasmonate-mediated antiherbivore defense responses in rice by silicon. *Proc. Natl. Acad. Sci. USA* **110**, E3631–E3639 (2013).
- Ziaee, M. & Ganji, Z. Insecticidal efficacy of silica nanoparticles against *Rhyzopertha dominica* F. and *Tribolium confusum* Jacquelin du Val. *J. Plant Prot. Res.* **56**, 250–256 (2016).
- La, V. H. et al. Salicylic acid improves drought-stress tolerance by regulating the redox status and proline metabolism in *Brassica rapa*. *Hortic. Environ. Biotechnol.* **60**, 31–40 (2019).
- Krajičková, A. & Mejstřík, V. The effect of fly ash particles on the plugging of stomata. *Environ. Pollut. A* **36**, 83–93 (1984).
- Burkhardt, J., Basi, S., Pariyar, S. & Hunsche, M. Stomatal penetration by aqueous solutions—an update involving leaf surface particles. *New Phytol.* **196**, 774–787 (2012).
- Amrullah, D. S. & Junaedi, A. Influence of nano-silica on the growth of rice plant (*Oryza sativa* L.). *Asian J. Agric. Res.* **9**, 33–37 (2015).
- Karunakaran, G. et al. Effect of nanosilica and silicon sources on plant growth promoting rhizobacteria, soil nutrients and maize seed germination. *IET Nanobiotechnol.* **7**, 70–77 (2013).
- Cameron, R. K., Pavia, N. K., Lamb, C. J. & Dixon, R. A. Accumulation of salicylic acid and *PR-1* gene transcripts in relation to the systemic acquired resistance (SAR) response induced by *Pseudomonas syringae* pv. *tomato* in *Arabidopsis*. *Physiol. Mol. Plant Pathol.* **55**, 121–130 (1999).
- Malamy, J., Carr, J. P., Klessig, D. F. & Raskin, I. Salicylic acid: a likely endogenous signal in the resistance response of tobacco to viral infection. *Science* **250**, 1002–1004 (1990).
- Fautoux, F., Chain, F., Belzile, F., Menzies, J. G. & Bélanger, R. R. The protective role of silicon in the *Arabidopsis*-powdery mildew pathosystem. *Proc. Natl. Acad. Sci. USA* **103**, 17554–17559 (2006).
- Jiang, N., Fan, X., Lin, W., Wang, G. & Cai, K. Transcriptome analysis reveals new insights into the bacterial wilt resistance mechanism mediated by silicon in tomato. *Int. J. Mol. Sci.* **20**, 761 (2019).

48. Lavers, A. *Guidelines on Good Practice for Ground Application of Pesticides* (Food and Agriculture Organization of the United Nations, 2001).
49. Schreiber, L. Polar paths of diffusion across plant cuticles: new evidence for an old hypothesis. *Ann. Bot.* **95**, 1069–1073 (2005).
50. Kookana, R. S. et al. Nanopesticides: guiding principles for regulatory evaluation of environmental risks. *J. Agric. Food Chem.* **62**, 4227–4240 (2014).
51. Kah, M., Tufenkji, N. & White, J. C. Nano-enabled strategies to enhance crop nutrition and protection. *Nat. Nanotechnol.* **14**, 532–540 (2019).
52. Bourquin, J. et al. Biodistribution, clearance, and long-term fate of clinically relevant nanomaterials. *Adv. Mater.* **30**, e1704307 (2018).
53. Mebert, A. M., Baghole, C. J., Desimone, M. F. & Maysinger, D. Nanoengineered silica: properties, applications and toxicity. *Food Chem. Toxicol.* **109**, 753–770 (2017).

Publisher's note Springer Nature remains neutral with regard to jurisdictional claims in published maps and institutional affiliations.

© The Author(s), under exclusive licence to Springer Nature Limited 2020

Methods

Plant growth conditions. *A. thaliana* seeds were grown on Jiffy soil substrates (powered by Tref, Jiffy Products International). Two *A. thaliana* strains were grown: wild-type Columbia (Col-0) plants that carry an *RPS2* locus responsible for the recognition of *P. syringae* strains expressing the avirulent gene *avrRpt2* (refs. 28,29) and an *A. thaliana* mutant defective in SA biosynthesis (*sid2* (ref. 36)). The seeds sown on the soil were kept at 4 °C for 2 d and then transferred to the growth chamber (RMC Tableaux SA). The plants were grown in a 12 h photoperiod with 60% relative humidity, with a day temperature of 22 °C and a night temperature of 18 °C (photon flux density, 100 $\mu\text{mol m}^{-2} \text{s}^{-1}$). The transplanted seedlings were covered with transparent plastic domes for 2–3 d to allow the seedlings to adapt to the new soil. Four- to five-week-old plants were used in the experiments, because previous experiments had shown that under the abovementioned growth conditions, this is the optimal age of the plant to induce SAR³⁴.

Culture of *P. syringae* pv. *tomato*. *P. syringae* pv. *tomato* bacteria were prepared by inoculating a single colony in 10 ml King's B medium (1.5 g K₂HPO₄, 1.5 g MgSO₄·7H₂O, 20 g tryptone and 10 ml glycerol per litre of water; Sigma-Aldrich; purity ≥99%) containing the appropriate antibiotics. A virulent and an avirulent strain of *P. syringae* were grown: *P. syringae* DC3000 (virulent *P. syringae*) and *P. syringae* DC3000 expressing the avirulent gene *avrRpt2* recognized by the *A. thaliana* *RPS2* locus and inducing SAR (avirulent *P. syringae*). The virulent *P. syringae* bacteria strain served to induce a strong infection with *P. syringae* in the plants. The avirulent *P. syringae* strain served as a positive control to induce SAR and thus an actively suppressed bacterial growth in the *A. thaliana* plants via recognition of the bacterial *avrRpt2* gene by the plant's *RPS2* gene (refer to ref. 29 for a detailed description of the pathosystem). The virulent *P. syringae* was grown with rifampicin (25 $\mu\text{g ml}^{-1}$) and the avirulent *P. syringae* was grown with kanamycin (50 $\mu\text{g ml}^{-1}$) or rifampicin (25 $\mu\text{g ml}^{-1}$). After overnight incubation in a shaker at 28 °C in the dark (Kuhner LT-W Lab Therm Table Top Incubator Shaker, Adolf Kühner AG), the cells were centrifuged at 3,000 r.p.m. for 10 min, and the pellet was suspended in 10 mM MgCl₂. The cell density was calculated by measuring the light absorption of the liquid culture using a spectrophotometer (BioPhotometer, Eppendorf) at the absorption wavelength of 600 nm and by counting the colonies plated on King's B agar (raw data are publicly available³⁵).

Inoculation procedures for local disease resistance. For a local disease resistance assay, three leaves per *A. thaliana* plant were inoculated with the virulent *P. syringae* bacteria, and the plants were incubated under the standard *A. thaliana* growth conditions described above. The inoculation with the virulent *P. syringae* bacteria was operationally defined as 0 d post inoculation (dpi). After inoculation, leaf discs (4 mm) were collected from the inoculated leaves at 0 and 3 dpi using a cork borer (three leaf discs from different plant leaves per sample). The leaf discs were ground and homogenized with pestles in 10 mM MgCl₂ and the undiluted (0 dpi) or the 1,000-fold diluted (3 dpi) homogenates were plated on King's B agar plates (King's B medium as above with 15 g l⁻¹ agar). The plates were incubated at 28 °C in the dark for 48 h. Then the bacterial colonies were counted (raw data are publicly available³⁵).

Inoculation procedures for SAR assays. For an SAR assay, three leaves of four- to five-week-old wild-type Col-0 plants were infiltrated with 10 mM MgCl₂ (negative control) or the avirulent *P. syringae* bacteria at 10⁶ colony-forming units (CFU) per millilitre in 10 mM MgCl₂ (positive control). After 48 h, the distal leaves were inoculated with the virulent *P. syringae* bacteria (10⁵ CFU ml⁻¹). The inoculation with the virulent *P. syringae* bacteria was operationally defined as 0 dpi. Leaf discs (4 mm) were collected from the distal leaves at 0 and 3 dpi using a cork borer (three leaf discs from different plant leaves were analysed three times for each treatment). The leaf discs were ground in 10 mM MgCl₂, and the undiluted (0 dpi) or 1,000-fold diluted (3 dpi) homogenates were plated on King's B agar and incubated at 28 °C for 48 h in the dark (SalvisLab incubator). Then the bacterial colonies were counted (raw data are publicly available³⁵). For details about this procedure, refer to ref. 18.

Plant treatments. The SiO₂ NPs (25, 100, 400 and 1,600 mg SiO₂ l⁻¹ at pH 7) and Si(OH)₄ (5, 20, 80, 100, 320, 640 and 2,560 mg SiO₂ l⁻¹ at pH 7 from an aqueous potassium silicate stock solution; K₂O:SiO₂ of 1:2.60; SiO₂ content, 20.8 wt%; MonDroguiste) were prepared in sterile, distilled water in HEPES buffer (1 mM, pH 7, 99.5%; Sigma-Aldrich). The Si(OH)₄ concentrations were expressed in mg SiO₂ l⁻¹ to facilitate a direct comparison of the effects of dissolved Si(OH)₄ and solid SiO₂ NPs without having to take into account the different molecular weights.

For the local disease resistance assay, the plants were sprayed with these chemicals 24 h before inoculation with virulent *P. syringae*. For the SAR assays, all these chemicals were injected abaxially (from the bottom of the leaf) into *Arabidopsis* plant leaves 2 d before inoculation using 1 ml needleless sterile disposable syringes.

SiO₂ NPs and subcellular distribution within the leaf. The SiO₂ NPs were synthesized and characterized according to a previously established procedure^{31,32} adapted from an earlier work³⁶. Briefly, one equivalent of tetraethyl orthosilicate

(10 ml, >99%; Sigma-Aldrich) was added to an equilibrated reaction mixture at 70 °C containing two equivalents of ultrapure water (Milli-Q, 18.2 MΩ arrium 611 DI, Sartorius Stedim Biotech), and absolute ethanol (81 ml) as a solvent under basic conditions (2.93 ml of 25% NH₃). The particles resulting after 3 h of hydrolysis and polycondensation of tetraethyl orthosilicate were washed by three steps of centrifugation (15,000 $\times g$ for 15 min, where g is the Earth's gravitational acceleration) in ultrapure water and five or more steps of dialysis through a membrane with a 14 kDa molecular weight cutoff (regenerated cellulose, Carl Roth). Several batches of particles with hydrodynamic diameter in the range of 64.8–76.7 nm were prepared using an identical procedure to prevent artefacts due to suspension aging (size variability between batches, 5.2 nm). DLS was used to quantify the hydrodynamic particle size and surface charge of the diluted samples (1% v/v; NanoBrook Particle Size Analyzer 90Plus, Brookhaven; scattering angle, 90° at 1 min acquisition; raw data are publicly available³⁵). Inductively coupled plasma-optical emission spectroscopy and gravimetry served to quantify the SiO₂ concentration (methods described in ref. 31).

For the particle characterization and to analyse the effects of SiO₂ NPs, Si(OH)₄ and control treatments in the leaves, we used TEM. The particle size distribution was established using the ImageJ software (version 1.52n) analysis of the TEM micrographs (raw data are publicly available³⁵). The plants were pre-fixed in 4% glutaraldehyde solution, gently stained in the dark with 1% OsO₄ solution that was centrifuged beforehand to remove potential precipitates, dehydrated using an ethanol series and embedded in polymer resin (AGAR Low Viscosity Kit, Plano) without further staining according to a procedure described in detail in ref. 57. The correct position of the stomata to cut the cross-sections were identified by light microscopy examination of semi-thin resin sections before ultramicrotoming. The TEM images were taken on an FEI Tecnai Spirit instrument at an acceleration voltage of 120 kV (resolution, 2,048 \times 2,048 pixels; Veleta CCD camera, Olympus). Besides the cropping and adjustment of brightness and contrast, the micrographs were not further processed; unprocessed raw data are publicly available³⁵.

DNA extraction. The plant leaf samples (five leaf discs from different inoculated plant leaves per sample) were frozen in liquid nitrogen and were homogenized using a ceramic mortar and pestle. The total DNA was extracted with a Plant DNA Mini Kit (peqlab, VWR). More information about the sample preparation is available in Supplementary Information, 'Details on DNA extraction'.

RNA extraction and complementary DNA synthesis. The plant leaf samples (ten leaf discs taken from different infiltrated plant leaves per sample) were flash frozen in liquid nitrogen, and the total RNA was extracted with the Spectrum Plant Total RNA Kit (Sigma Life Science). One microgram of the total RNA was used for complementary DNA synthesis using the Omniscript Reverse Transcription Kit (Qiagen). More information about the sample preparation is available in the Supplementary Information, 'Details on RNA extraction and complementary DNA synthesis'.

qPCR. To validate the SAR response based on the bacterial colony counts, the bacteria were also quantified via the outer membrane protein *oprF* gene of *P. syringae* in the inoculated leaves (raw data are publicly available³⁵) based on a previously established method^{18,33}. For this bacterial DNA quantification, a reaction mixture for qPCR was prepared with 7.5 μl of 2× SensiMix SYBR Hi-ROX Mastermix (no. QT605-05, Bioline, Meridian Bioscience), 5 μl plant DNA and 0.5 μl of each primer (Supplementary Table 1) at a concentration of 10 μM in a final volume replenished with water to 15 μl in magnetic induction cycler (Mic tubes (Bio Molecular Systems). The runs were performed on a Mic qPCR machine (Bio Molecular Systems). The conditions for the qPCR were as follows: initial denaturation for 10 min at 95 °C followed by 40 cycles (95 °C for 15 s, 62 °C for 1 min and 72 °C for 30 s). The final PCR products were analysed by a melting point analysis. The qPCR analysis software for the melting curve analysis and amplification efficiency calculation was micPCR v. 2.8.13 (Bio Molecular Systems). This software is designed to meet the minimum information for publication of quantitative real-time PCR experiments (MIQE)³⁸ specifications and automatically performs the qPCR analysis based on the real-time runs. Five leaf discs from different plant leaves were sampled for each replicate, frozen in liquid nitrogen and immediately processed for DNA extraction. The bacterial DNA levels of the bacterial *oprF* gene in *Arabidopsis* plants were calculated using At4g26410 (*expG*) as a reference gene³³ and the comparative cycle threshold method ($2^{(-\Delta\Delta C_t)}^{39}$).

For oxidative stress and SA-responsive plant transcript levels, leaf discs were flash frozen in liquid nitrogen and stored at -80 °C for <24 h before being processed for RNA extraction and complementary DNA synthesis. Three independent technical replicates (ten leaf discs taken from different plant leaves) were used per treatment. The reaction mixture for RT-qPCR contained 7.5 μl of 2× SensiMix SYBR Hi-ROX Mastermix (no. QT605-05, Bioline, Meridian Bioscience), 5 μl of complementary DNA (corresponding to 25 ng RNA) and 0.5 μl of each primer (Supplementary Table 1) at a concentration of 10 μM in a final volume replenished with water to 15 μl in Mic tubes (Bio Molecular Systems). Runs were performed on a Mic qPCR machine (Bio Molecular Systems). The conditions for the qPCR and the analysis of the final PCR products by melting point analysis were analogous to the above bacterial DNA quantification. The final PCR products were

analysed by a melting point analysis. The transcript levels of the oxidative stress marker (*At3g46230; HSP17.4C1*)³⁴ and the SA-responsive genes *AtPR-1* and *AtPR-5* in *Arabidopsis* plants were calculated with *At4g26410 (expG)* as the reference gene⁶⁰ and the comparative cycle threshold method ($2^{(-\Delta\Delta C_t)}$) as mentioned above.

The *expG* gene was selected because another study⁶⁰ specifically recommended *expG* as one of the top five reference genes to be used in biotic stress studies due to its high stability under such conditions. This high stability was confirmed in a previous work of our laboratory⁶¹ and another work¹³. In the present study, the stable expression of *expG* is reflected in the very small variation in the cycle in which fluorescence can be detected in qPCR termed quantitation cycle (C_q) for *expG*. For example, in the *PR-1* expression experiments (Fig. 6c), the average C_q ranged from 23.19 to 23.93 for all the different testing conditions, with an average relative error of only 0.63% (ref. ⁵⁵). All the amplification efficiencies were very close to two and with good comparability between the reference gene and the target gene. For example, in Fig. 6c, the average amplification efficiency of *expG* and *AtPR-1* across all the different treatment conditions (1.949 ± 0.011 versus 1.962 ± 0.027 , averages \pm standard deviations) differed by only 0.7% (ref. ⁵⁵). All the statistical tests hereinafter were performed using the IBM SPSS Statistics software (version 22).

Ecotoxicity of SiO₂ NPs and Si(OH)₄ to *C. elegans* larvae. The ecotoxicity assays were conducted on the larval stage one (L1) nematodes of the *C. elegans* wild-type (ancestral; N2) genotype. Synchronized *C. elegans* larvae were grown according to a previously established protocol⁶² (raw data are publicly available⁵⁵). A known number of larvae (~70) per replicate were then exposed to 0, 25, 125, 250, 500, 750, 1,000, 1,500 or 2,000 mg SiO₂ l⁻¹ of SiO₂ NPs or Si(OH)₄ in 96-well plates (Corning Costar no. 3596). A 0.1% Na₃N solution served as the positive control. As a food source for the nematodes, the wells contained 10 µl of living *Escherichia coli* (strain OP50; final optical density at 600 nm and 1 a.u.; $\sim 5 \times 10^6$ cells ml⁻¹). The total volume per well was 100 µl, and the final pH installed in the phosphate-buffered saline test solutions was 7.4. After incubating the nematodes at 20 °C for 48 h in the dark, the surviving larvae were counted under a stereo microscope at $\times 20$ magnification. The resulting number of mobile nematode larvae was subtracted from the initially incubated number of larvae to calculate the percentage of immobile nematodes. The EC₅₀ values were calculated using a numerically fitted standard log-logistic dose-response model (Levenberg–Marquardt iteration algorithm, Origin 2016, build 9.3.2.903, OriginLab; Supplementary Fig. 3). The experiment comprised 12 biological replicates for each treatment and was repeated twice with comparable results.

Data availability

The datasets that support the findings of the current study are available in the Zenodo repository with the identifier <https://doi.org/10.5281/zenodo.4131137>. Additional data related to this study are available from the corresponding authors upon reasonable request.

References

54. Chen, Z. et al. Pseudomonas syringae type III effector AvrRpt2 alters *Arabidopsis thaliana* auxin physiology. *Proc. Natl. Acad. Sci. USA* **104**, 20131–20136 (2007).
55. El-Shetehy, M. et al. Silica nanoparticles enhance disease resistance in *Arabidopsis* plants—raw data. *Zenodo* <https://doi.org/10.5281/zenodo.4131137> (2020).
56. Stöber, W., Fink, A. & Bohn, E. Controlled growth of monodisperse silica spheres in the micron size range. *J. Colloid Interface Sci.* **26**, 62–69 (1968).
57. Stegemeier, J. P. et al. Speciation matters: bioavailability of silver and silver sulfide nanoparticles to alfalfa (*Medicago sativa*). *Environ. Sci. Technol.* **49**, 8451–8460 (2015).
58. Bustin, S. A. et al. The MIQE guidelines: minimum information for publication of quantitative real-time PCR experiments. *Clin. Chem.* **55**, 611–622 (2009).
59. Rao, X., Huang, X., Zhou, Z. & Lin, X. An improvement of the $2^{-\Delta\Delta C_t}$ method for quantitative real-time polymerase chain reaction data analysis. *Biostat. Bioinforma. Biomath.* **3**, 71 (2013).
60. Czechowski, T., Stitt, M., Altmann, T., Udvardi, M. K. & Scheible, W.-R. Genome-wide identification and testing of superior reference genes for transcript normalization in *Arabidopsis*. *Plant Physiol.* **139**, 5–17 (2005).
61. Tomczynska, I., Stumpe, M. & Mauch, F. A conserved RxLR effector interacts with host RABA-type GTPases to inhibit vesicle-mediated secretion of antimicrobial proteins. *Plant J.* **95**, 187–203 (2018).
62. Joller, C. et al. S-methyl methanethiosulfonate: promising late blight inhibitor or broad range toxin? *Pathogens* **9**, 496 (2020).

Acknowledgements

M.E.-S. was supported by the Swiss State Secretariat for Education, Research and Innovation by a Swiss Government Excellence Scholarship for Foreign Scholars. F.S. and M.M. were supported by the Swiss National Science Foundation under the Ambizione grant ‘Enhancing Legume Defenses’ (161817) and Innosuisse (project 38515.1 IP-EE). We are grateful to N. Schäppi for his help with the graphic design and M. Schorderet for excellent technical assistance with micromotoring. This work benefitted from support from the Swiss National Science Foundation through the National Center of Competence in Research Bio-Inspired Materials. This research was also supported by the Adolphe Merkle Foundation and the University of Fribourg.

Author contributions

M.E.-S., F.S. and F.M. conceived and designed the study. F.S. led the team, rationally designed the SiO₂ NPs to induce optimal plant defence, performed initial germination tests to establish the dosing regimen, contributed to the mechanistic understanding of silica and with plant TEM and has drawn the artwork. M.M. synthesized and characterized the SiO₂ NPs. A.M. cultured the *Arabidopsis* plants and conducted the *C. elegans* experiments. D.R. provided access to his micromotome and a technician that trained F.S. in micromotoring. M.E.-S. performed all the *Arabidopsis* experiments and their statistical evaluation and wrote the manuscript draft with contributions by F.S. (figures and text) and F.M. (text). F.M. contributed to the mechanistic understanding of the gene expression results and molecular mechanisms of SAR. The manuscript was critically reviewed by A.P.-F., B.R.-R. and D.R. All the co-authors read and approved the manuscript before submission.

Competing interests

Any opinions, findings, conclusions or recommendations expressed in this material are those of the authors and do not necessarily reflect the views of the Swiss National Science Foundation or the government. This work has not been subjected to Swiss National Science Foundation review, and no official endorsement should be inferred. F.S. and M.M. have a patent pending on a SiO₂ NP plant growth enhancer. F.S. was supported by Innosuisse (project no. 38515.1 IP-EE). Other than that, the authors have declared no conflict of interest and are responsible for the content and writing of the article.

Additional information

Supplementary information is available for this paper at <https://doi.org/10.1038/s41565-020-00812-0>.

Correspondence and requests for materials should be addressed to M.E.-S. or F.S.

Peer review information *Nature Nanotechnology* thanks Rai Kookana and the other, anonymous, reviewer(s) for their contribution to the peer review of this work.

Reprints and permissions information is available at www.nature.com/reprints.